Localized surface plasmon enhanced quantum efficiency of InGaN/GaN quantum wells by Ag/SiO_2 nanoparticles

Lee-Woon Jang,[1] Dae-Woo Jeon,[1] Trilochan Sahoo,[1] Dong-Seob Jo,[1] Jin-Woo Ju,[2] Seung-jae Lee,[2] Jong-Hyeob Baek,[2] Jin-Kyu Yang,[3] Jung-Hoon Song,[4] Alexander Y. Polyakov,[1] and In-Hwan Lee[1,*]

[1]*School of Advanced Materials Engineering and Research Center of Advanced Materials Development, Chonbuk National University, Jeonju 561-756, South Korea*
[2]*LED device team, Korea Photonics Technology Institute, Gwangju 500-779, South Korea*
[3]*Department of Optical Engineering, Kongju National University, Kongju, Chungnam 314, 701, South Korea*
[4]*Department of Physics, Kongju National University, Kongju, Chungnam 314-701, South Korea*
[*]*ihlee@jbnu.ac.kr*

Abstract: Optical properties of InGaN/GaN multi-quantum-well (MQW) structures with a nanolayer of Ag/SiO_2 nanoparticle (NP) on top were studied. Modeling and optical absorption (OA) measurements prove that the NPs form localized surface plasmons (LSP) structure with a broad OA band peaked near 440–460 nm and the fringe electric field extending down to about 10 nm into the GaN layer. The presence of this NP LSP electrical field increases the photoluminescence (PL) intensity of the MQW structure by about 70% and markedly decreases the time-resolved PL (TRPL) relaxation time due to the strong coupling of MQW emission to the LSP mode.

OCIS codes: (240.6680) Surface plasmons; (250.5230) Photoluminescence; (250.5590) Quantum-well, -wire and -dot devices.

References and links

1. W. L. Barnes, A. Dereux, and T. W. Ebbesen, "Surface plasmon subwavelength optics," Nature **424**(6950), 824–830 (2003).
2. P. Andrew and W. L. Barnes, "Energy transfer across a metal film mediated by surface plasmon polaritons," Science **306**(5698), 1002–1005 (2004).
3. R. Bardhan, N. K. Grady, and N. J. Halas, "Nanoscale control of near-infrared fluorescence enhancement using Au nanoshells," Small **4**(10), 1716–1722 (2008).
4. F. Tam, G. P. Goodrich, B. R. Johnson, and N. J. Halas, "Plasmonic enhancement of molecular fluorescence," Nano Lett. **7**(2), 496–501 (2007).
5. P. Nagpal, N. C. Lindquist, S. H. Oh, and D. J. Norris, "Ultrasmooth patterned metals for plasmonics and metamaterials," Science **325**(5940), 594–597 (2009).
6. A. V. Akimov, A. Mukherjee, C. L. Yu, D. E. Chang, A. S. Zibrov, P. R. Hemmer, H. Park, and M. D. Lukin, "Generation of single optical plasmons in metallic nanowires coupled to quantum dots," Nature **450**(7168), 402–406 (2007).
7. E. Dulkeith, T. Niedereichholz, T. Klar, J. Feldmann, G. von Plessen, D. Gittins, K. Mayya, and F. Caruso, "Plasmon emission in photoexcited gold nanoparticles," Phys. Rev. B **70**(20), 205424 (2004).
8. C. Langhammer, M. Schwind, B. Kasemo, and I. Zoric, "Localized surface plasmon resonances in aluminum nanodisks," Nano Lett. **8**(5), 1461–1471 (2008).
9. K. A. Willets and R. P. Van Duyne, "Localized surface plasmon resonance spectroscopy and sensing," Annu. Rev. Phys. Chem. **58**(1), 267–297 (2007).
10. M. W. Knight, N. K. Grady, R. Bardhan, F. Hao, P. Nordlander, and N. J. Halas, "Nanoparticle-mediated coupling of light into a nanowire," Nano Lett. **7**(8), 2346–2350 (2007).
11. A. L. Falk, F. H. L. Koppens, C. L. Yu, K. Kang, N. de Leon Snapp, A. V. Akimov, M. H. Jo, M. D. Lukin, and H. Park, "Near-field electrical detection of optical plasmons and single-plasmon sources," Nat. Phys. **5**(7), 475–479 (2009).
12. Y. Zhang, A. Barhoumi, J. B. Lassiter, and N. J. Halas, "Orientation-preserving transfer and directional light scattering from individual light-bending nanoparticles," Nano Lett. **11**(4), 1838–1844 (2011).
13. S. F. Chichibu, A. Uedono, T. Onuma, B. A. Haskell, A. Chakraborty, T. Koyama, P. T. Fini, S. Keller, S. P. Denbaars, J. S. Speck, U. K. Mishra, S. Nakamura, S. Yamaguchi, S. Kamiyama, H. Amano, I. Akasaki, J. Han,

#156569 - $15.00 USD Received 8 Nov 2011; revised 28 Dec 2011; accepted 2 Jan 2012; published 17 Jan 2012

and T. Sota, "Origin of defect-insensitive emission probability in In-containing (Al,In,Ga)N alloy semiconductors," Nat. Mater. **5**(10), 810–816 (2006).
14. M. K. Kwon, J. Y. Kim, B. H. Kim, I. K. Park, C. Y. Cho, C. C. Byeon, and S. J. Park, "Surface-plasmon-enhanced light-emitting diodes," Adv. Mater. (Deerfield Beach Fla.) **20**(7), 1253–1257 (2008).
15. D. M. Yeh, C. Y. Chen, Y. C. Lu, C. F. Huang, and C. C. Yang, "Formation of various metal nanostructures with thermal annealing to control the effective coupling energy between a surface plasmon and an InGaN/GaN quantum well," Nanotechnology **18**(26), 265402 (2007).
16. K. Okamoto, I. Niki, A. Shvartser, Y. Narukawa, T. Mukai, and A. Scherer, "Surface-plasmon-enhanced light emitters based on InGaN quantum wells," Nat. Mater. **3**(9), 601–605 (2004).
17. P. Mulvaney, "Surface plasmon spectroscopy of nanosized metal particles," Langmuir **12**(3), 788–800 (1996).
18. N. C. Greenham, X. Peng, and A. P. Alivisatos, "Charge separation and transport in conjugated-polymer/semiconductor-nanocrystal composites studied by photoluminescence quenching and photoconductivity," Phys. Rev. B Condens. Matter **54**(24), 17628–17637 (1996).
19. W. Wang, Z. Li, B. Gu, Z. Zhang, and H. Xu, "Ag-SiO_2 core-shell nanoparticles for probing spatial distribution of electromagnetic field enhancement via surface-enhanced Raman scattering," ACS Nano **3**(11), 3493–3496 (2009).
20. K. Xu, J. X. Wang, X. L. Kang, and J. F. Chen, "Fabrication of antibacterial monodispersed Ag-SiO_2 core-shell nanoparticles with high concentration," Mater. Lett. **63**(1), 31–33 (2009).
21. F. Gao, Q. Lu, and D. Zhao, "Controllable assembly of ordered semiconductor Ag_2S nanostructures," Nano Lett. **3**(1), 85–88 (2003).
22. J. K. Yang, I. K. Hwang, M. K. Seo, S. H. Kim, and Y. H. Lee, "Plasmon-suppressed vertically-standing nanometal structures," Opt. Express **16**(3), 1951–1957 (2008).
23. P. B. Johnson and R. W. Christy, "Optical contrast of the noble metals," Phys. Rev. B **6**(12), 4370–4379 (1972).
24. J. A. Dionne, L. A. Sweatlock, H. A. Atwater, and A. Polman, "Planar metal plasmon waveguides: frequency-dependent dispersion, propagating, localization, and loss beyond the free electron model," Phys. Rev. B **72**(7), 075405 (2005).
25. W. Sigle, J. Nelayah, C. T. Koch, and P. A. van Aken, "Electron energy losses in Ag nanoholes--from localized surface plasmon resonances to rings of fire," Opt. Lett. **34**(14), 2150–2152 (2009).
26. W. L. Barnes, "Surface plasmon-polariton length scale: a route to sub-wavelength optics," J. Opt. A, Pure Appl. Opt. **8**(4), S87–S93 (2006).
27. M. I. Stockman, "Nanoplasmonics: the physics behind the applications," Phys. Today 2011 **64**(2), 39 (2011).
28. D. M. Graham, P. Dawson, G. R. Chabrol, N. P. Hylton, D. Zhu, M. J. Kappers, C. McAleese, and C. J. Humphreys, "High photoluminescence quantum efficiency InGaN multiple quantum well structures emitting at 380nm," J. Appl. Phys. **101**(3), 033516 (2007).
29. A. H. Chin, T. S. Ahn, H. Li, S. Vaddiraju, C. J. Bardeen, C. Z. Ning, and M. K. Sunkara, "Photoluminescence of GaN nanowires of different crystallographic orientations," Nano Lett. **7**(3), 626–631 (2007).
30. J. V. Foreman, J. Li, H. Peng, S. J. Choi, H. O. Everitt, and J. Liu, "Time-resolved investigation of bright visible wavelength luminescence from sulfur-doped ZnO nanowires and micropowders," Nano Lett. **6**(6), 1126–1130 (2006).
31. C. Y. Cho, K. S. Kim, S. J. Lee, M. K. Kwon, H. D. Ko, S. T. Kim, G. Y. Jung, and S. J. Park, "Surface Plasmon-enhanced light-emitting diodes with silver nanoparticles and SiO_2 nano-disks embedded in p-GaN," Appl. Phys. Lett. **99**(4), 041107 (2011).

1. Introduction

Surface plasmons (SP) are of great interest to many scientists in various research fields due to the extremely strong light concentration in sub-wavelength-thick metallic structures [1, 2]. The nanometre-scale metallic particles are used to obtain the phase matching and strong enhancement of the local electric field due to what is known as localized surface plasmons (LSPs) phenomena [3–12]. Recently, LSPs have attracted great interest in light-emitting-diodes (LEDs) applications. In conventional LEDs, the emission efficiency depends on the optical extraction efficiency and internal quantum efficiency. The latter is limited by several factors, such as a high threading dislocation density contributing to the high density of non-radiative recombination centers and the quantum confined Stark effect due to strong polarization fields in GaN-based quantum wells. The former is severely handicapped by the high refractive index of GaN leading to a low angle of total internal reflection and hence a low portion of light that can be extracted from the active region of LEDs [13].

However, the presence of metallic nano-particles pattern close to the multiple quantum well (MQW) structure enables the ready excitation of LSP that converts the energy dissipated in non-radiative recombination processes to the energy of photons with the wavelength close to the wavelength of the MQW recombination photons.

This distinctive phenomenon has been intensely studied in InGaN/GaN based MQW structure using various metals, such as Ag, Au, Al [14–16]. Okamoto et al. have reported

#156569 - $15.00 USD Received 8 Nov 2011; revised 28 Dec 2011; accepted 2 Jan 2012; published 17 Jan 2012

photoluminescence (PL) and internal quantum efficiency (IQE) enhancement by LSP coupling using Ag [16]. Yeh et al. have demonstrated that the emission peak could be tuned by controlling the size of Ag nano-particles (NPs) [15]. Similarly, EL enhancement by LSP coupling for Ag embedded sample was reported by Kwon et al [14]. From these recent reports it is clear that the metal nanostructures could play a significant role in improving the emission efficiency of MQW structure by LSP coupling. However, the metal nanostructures are affected by the geometry and separation of NPs [4]. Moreover, because the metal nanostructure is exposed to air during the device testing, operation and storage, the surface of metal nanostructures can be easily oxidized resulting in changes in the LSP resonance spectrum [17] and the emergence of additional energy loss channels [6, 18]. Hence, avoiding oxidation and energy loss of metal nanostructures are an important issue for SP–assisted LED studies. One of the keys to solving these problems is the use of metal nanostructures coated with a dielectric shell layer. The structure of metal core/insulator shell NPs was studied by many research groups [3,19] and they reported on the impact of the insulator shell on LSP properties and the behavior of NPs. Here we report on the application of the core/shell NPs to MQW structure and demonstrate their effect on the emission efficiency of devices.

In what follows we present the studies of the LSP phenomenon for core/shell NPs on InGaN/GaN MQW structure. To understand the LSP phenomena for core/shell NPs on MQW structure, we have first analyzed the LSP resonance of Ag/SiO_2-NPs by the full three-dimensional (3-D) finite-difference time-domain (FDTD) simulation. Conventional PL and time-resolved PL (TRPL) were employed to investigate the influence on optical characteristics. From the results of simulation and from experimental results, the PL enhancement and improvement of the IQE after NPs coating are attributed to the energy transfer from MQWs to Ag/SiO_2-NPs by LSP coupling.

2. Experimental methods

The InGaN/GaN MQWs structure was epitaxially grown by metal organic chemical vapor deposition (MOCVD) technique. Trimethylgallium (TMGa), trimethylindium (TMIn) and NH_3 were used as precursors for Ga, In and N, respectively. A thermal annealing of c-plane sapphire substrate was carried out at 1100 °C for 10 min, followed by the growth of a low temperature GaN buffer layer. A 400-nm-thick undoped GaN layer was grown at 1060 °C. Then, five pairs of InGaN/GaN MQWs were grown on high quality GaN epitaxial layer. The GaN barriers and InGaN wells were grown at temperatures of 850 °C and 750 °C, respectively. Finally, a 10-nm-thick undoped GaN layer was grown on it as a spacer layer.

The Ag/SiO_2 core/shell NPs were synthesized by sol-gel method. A typical preparation procedure is as follows. First, a 500mL beaker was filled with 180mL of aqueous solution including cetyl trimethyl ammonium bromide (CTAB, 0.145g) under vigorous magnetic stirring. Next, a prepared aqueous solution of silver nitrate (0.1M, 10mL) was added to the mixed solution. And then, 20mL of ascorbic acid in aqueous solution was added to the mixture solution slowly within 5 min. After the mixture was further stirred for 10 min, sodium hydroxide (0.1M) was added to accelerate the chemical reaction and the pH of the mixed solution was set at about 5. Subsequently, 50mL of ethanol and 1mL of tetraethoxysilane was added into the above-mentioned silver colloids. The solution was stirred for three more hours at room temperature (RT).

The full 3-D FDTD simulation was performed to understand the electric field distribution of Ag/SiO_2 NPs. In the spatially digitized numerical simulation, minimum spatial size (grid size) should be small enough to resolve the field distribution, and 1-nm resolution in space (1 nm^3 in volume) was maintained. The diameter of Ag NPs was taken as 60 nm and the thickness of the SiO_2 coating (n = 1.55) as 20 nm. The single Ag/SiO_2 core/shell was placed on top of GaN (n = 2.3). The broad dipole source (λ_c = 470 nm, $\Delta\lambda$ = 60 nm) was positioned 10 nm below the contact point of GaN and Ag/SiO_2-NPs which corresponds to the location of InGaN/GaN MQWs in our structures.

The morphology of the Ag/SiO_2 NPs was investigated by TEM (JEOL, JEM 2100F) and field emission scanning electron microscopy (FE-SEM, JEOL, S4500). For the conventional

#156569 - $15.00 USD Received 8 Nov 2011; revised 28 Dec 2011; accepted 2 Jan 2012; published 17 Jan 2012

photoluminescence, 325 nm line of a He–Cd laser (KIMMON ELECTRIC) was used as the excitation source with a power of 25 mW and the measurement was performed through back-side of sample. TRPL (using HORIBA Jobin Yvon) was performed under pulse excitation of the InGaN/GaN based LED (pulse width of ~5 ps, center wavelength of ~405 nm) and the signals were analyzed by a monochromater, a photomultiplier tube, a high speed photodetector and controller electronics. All decay lifetimes were calculated by the supplied software of Fluorescence Division.

3. Results and discussion

The morphology of the Ag/SiO_2-NPs was investigated by transmission electron microscopy (TEM). A typical TEM image of Ag/SiO_2-NPs synthesized by sol-gel method [20] is shown in Fig. 1. The Ag particle is clearly seen as a gray core completely covered by the SiO_2 shell. The size and morphology of the SiO_2 shell can be determined from the higher magnification image in Fig. 1(b). Selected-area electron diffraction (SAED) pattern of Fig. 1(c) confirmed the presence of crystalline Ag core [21]. For core/shell NPs, estimated size of Ag NPs was 30–50 nm and the thickness of the SiO_2 shell was about 20 nm. 10 ml of the Ag/SiO_2-NP colloidal solution was directly coated on the surface of the InGaN/GaN MQW structure by drop casting and drying at 100 °C.

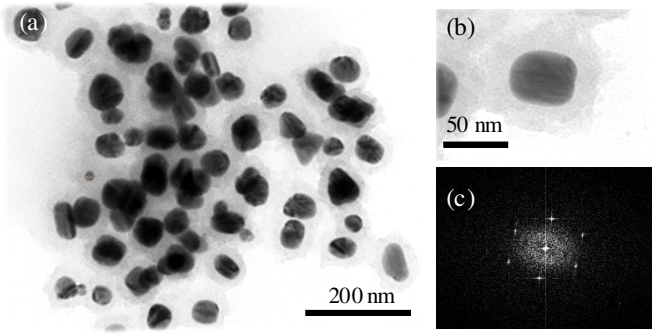

Fig. 1. TEM images (a, b) of the Ag/SiO_2 NPs synthesized by sol-gel method. SAED pattern take from the Ag core in the TEM image (c).

The schematic structure of the Ag/SiO_2-NP-coated InGaN/GaN MQW is shown in Fig. 2. The Ag/SiO_2-NPs was directly coated on the surface of the MQW structure by drop casting and drying. The inset shows the SEM image of Ag/SiO_2-NPs on the surface of MQW structure after coating.

In the LSP resonance, it is known that the emission in the near field of NPs is strongly enhanced relative to the incident optical wavelength [4]. In order to obtain the efficient energy transfer, the penetration depth of the LSP electric field into dielectric (GaN) is regarded as an important factor [14–16]. From the equation of effective length for energy transfer given in Ref. 16, the effective length for MQW-LSP coupling at the emission energy of 2.7 eV (459.2 nm; corresponding to the wavelength of our blue MQW device) is estimated at about 42 nm. However, this equation is applicable for a thin metal film and is not appropriate for core/shell NPs. Here, to calculate the effective length for energy transfer of the MQW-LSP resonance of Ag/SiO_2-NPs, the 3-D FDTD simulation was adopted. The optical properties of Ag NPs near emission energy (460 nm) were determined using the Drude equation and the data in Ref [22, 23].

#156569 - $15.00 USD Received 8 Nov 2011; revised 28 Dec 2011; accepted 2 Jan 2012; published 17 Jan 2012

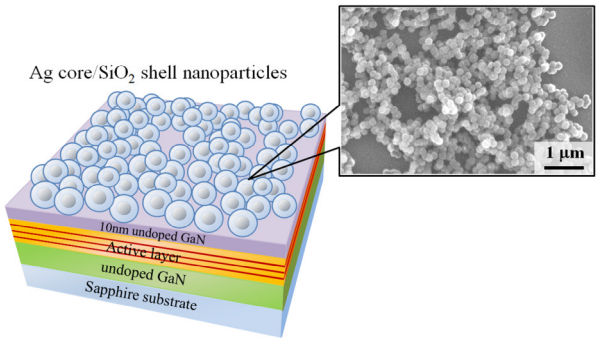

Fig. 2. Schematic sample structure of the Ag/SiO_2 NPs coated InGaN/GaN MQWs. The inset shows SEM image of surface after Ag/SiO_2 NPs coating.

Figures 3(a), 3(b), and 3(c) shows the electric field distribution of the resonant wavelength of the LSP mode for the cases of a single NP, 3 NPs, and 7 NPs. First, we investigate the behavior of single Ag/SiO_2-NP (Fig. 3(a)). The electric field of LSP mode is strongly confined near the surface of NPs and exponentially decays in the GaN. The intensity profiles for different numbers of NPs in the cluster for the wavelength near the resonance are shown in Fig. 3(d) for the direction along the z-axis. The effective length of the energy transfer is defined as the length from the metal surface to the position where the electric intensity decays by 1/e times of its maximum intensity [24]. From the result of numerical calculation shown in Fig. 3(d), the effective length for single Ag/SiO_2-NP is estimated as close to 8 nm. However, the resonance of NPs is strengthened through increasing the number of NPs (Fig. 3(b) and 3(c)) owing to the interaction between individual NPs [25]. As evident from Fig. 3(d), the decay length of electric field for three and seven NPs is higher than for single NP and one also observes a change in the intensity profile. Contrary to the case of single Ag/SiO_2-NP, with increasing NP number (three and seven NPs) the calculated depth is increased to 15 nm and 18 nm with similar increases in resonance intensity.

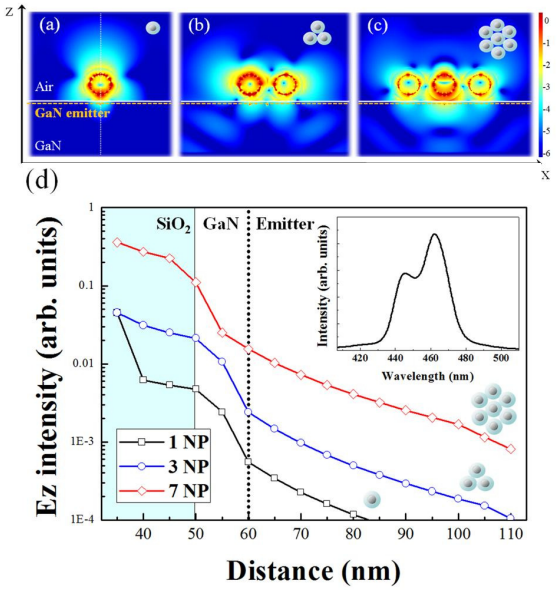

Fig. 3. Electric field distribution of the dipolar SP mode after source radiation. (a) single Ag/SiO_2-NP, (b) three Ag/SiO_2-NP, (c) seven Ag/SiO_2-NP and (d) resonance intensity of Ag/SiO_2-NPs along the z-axis. The Fig. 3(d) inset shows radiation spectra of Ag/SiO_2-NPs from FDTD simulation.

#156569 - $15.00 USD Received 8 Nov 2011; revised 28 Dec 2011; accepted 2 Jan 2012; published 17 Jan 2012

Compared to the calculated depth for the continuous metal layer, the penetration depth of NPs is very small and it is due to the divergence of the electric field around the NPs surface [26]. This short resonance depth of NPs can attenuate the energy transfer between LSP and MQWs. Moreover, the SiO_2 shell increases the distance from metal surface and leads to a relatively low luminescence enhancement [3, 6, 10, 16]. However, SiO_2 can provide a stability [3] and separation [4] of metal NPs and prevents the ohmic losses [5, 6, 18]. Mind though, that the LSP modes of NPs show the presence of a hot spot where extraordinarily strong concentration of the electric field intensity occurs, in contrast to SP of the continuous metal film. The local field enhancement of NPs is by a factor between 10^4 and 10^8 while the enhancement for the continuous metal film is by a factor between 10^2 and 10^4 [27]. Thus, for metal NPs, a much stronger enhancement of emission efficiency can be achieved [3, 6], albeit at the expense of a shorter effective penetration depth than for continuous films. The main features predicted by modeling are indeed observed in our experimental results.

Consider first the measured back-side PL spectra from the MQWs with and without Ag/SiO_2-NPs (Fig. 4). The Ag/SiO_2-NPs coated sample showed a remarkable increase in the PL by about 70% and a blue-shift [15] toward the LSP resonance compared with the uncoated sample. The measured by UV-Vis spectroscopy LSP resonance band in absorption shows for Ag/SiO_2-NPs a broad peak centered near 440 nm (Fig. 4, right axis), in reasonable agreement with the resonance wavelength obtained by FDTD simulation for the Ag/SiO_2-NPs by FDTD simulation (Fig. 3(b) inset) [14, 16]. This spectral region is well matched with the wavelength of blue MQW device, and the PL enhancement and wavelength shift of Ag/SiO_2-NPs coated sample can be anticipated due to the LSP coupling to the Ag core. The SiO_2-NPs coated sample without Ag core showed no wavelength shift and only 30% enhancement of PL intensity that we attribute to improved extraction efficiency (see Fig. 4).

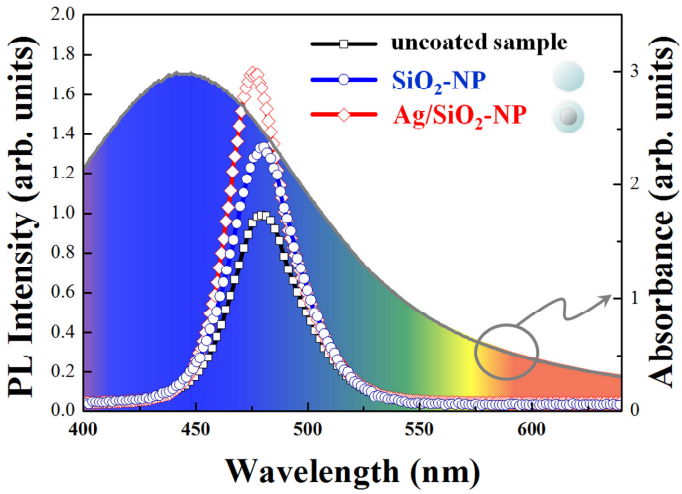

Fig. 4. Room temperature PL spectra from the reference, SiO_2-NPs and the Ag/SiO_2-NP coated sample, and the absorbance spectrum of the NPs.

The additional increase in PL intensity of Ag/SiO_2-NPs coated sample compared to SiO_2-NPs coated sample is attributed to increased IQE. The efficient LSP coupling increases IQE because the excited carriers transfer their energy to the LSP of the Ag NPs before being captured by non-radiative recombination centers, which leads to the enhancement of spontaneous emission rate of MQWs. This can be directly verified by low-temperature PL measurements [28]. The integrated IQE of uncoated sample (reference) and SiO_2-NPs coated sample was measured to be around 21% at RT by assuming IQE ≈100% at 10 K, while the integrated IQE of Ag/SiO_2-NP coated sample was estimated to be 30.5%.

#156569 - $15.00 USD Received 8 Nov 2011; revised 28 Dec 2011; accepted 2 Jan 2012; published 17 Jan 2012

Further insight is provided by TRPL peak intensity decay measurements whose results are presented in Fig. 5. It shows the carrier lifetime results of the reference, SiO_2-NPs and Ag/SiO_2-NPs coated sample at the peak emission wavelength.

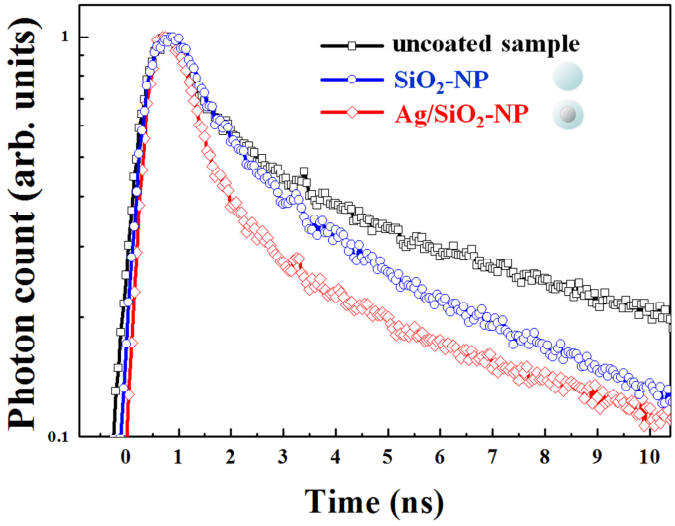

Fig. 5. Relaxation curves for the peak PL energy for the reference, SiO_2-NPs and the Ag/SiO_2-NP coated sample at room temperature.

These PL relaxation curves show a multi-stage decay behavior. Two characteristic decay times were generally observed. The fast decay time was attributed to exciton recombination while the long decay time was due to localized carrier recombination. For the case of strong LSP coupling, the life-time is related to the electron oscillation frequency which is much shorter than the relaxation time in conventional MQW LEDs [14, 15]. The TRPL analysis from fast decay regions revealed that the lifetimes of the reference and the SiO_2-NP coated samples were 1.38 ns and 1.05 ns, respectively. A slightly shorter life-time of the SiO_2-NP coated sample suggests the possibility of a surface trapping process. The SiO_2-NP coating can enhance nonradiative recombination processes at the SiO_2/GaN interface [29, 30]. In contrast to the uncoated and SiO_2-coated samples, the lifetime of Ag/SiO_2-NP coated sample was 480 ps. This shortest lifetime and enhanced PL of Ag/SiO_2-NP coated sample indicate that it is not a nonradiative relaxation process and that rather these effects are related to the increase in the spontaneous emission rate by the energy coupling of MQW-LSP.

4. Conclusion

We have demonstrated that the deposition of Ag/SiO_2 NPs on top of GaN/InGaN MQW structures increases the PL intensity by about 70% due to strong coupling of the MQW emission to LSP states formed by NPs. According to the FDTD simulation, the LSP resonance of NPs exhibits strongly confined field near the surface of Ag core. However, high enhancement factor of Ag/SiO_2-NPs can lead to the high efficiency LSP mediated LEDs. The improvement is due to increased value of IQE and photon extraction efficiency. Compared to the well documented case of IQE improvement due to metallic NP, core/shell structures, such as Ag/SiO_2-NPs, offer a high potential barrier for oxidation in the ambient atmosphere and should be less susceptible to degradation caused by this oxidation. The SiO_2 shells are also very efficient in preventing coagulation of nanoparticles during LED operation which is a serious concern for simple Ag NPs (detailed studies of the phenomenon will be presented in a separate paper). However, because the relatively short penetration depth of LSP electric field of NPs gives rise to the limitations of luminescence enhancement efficiency, in practical LSP enhanced LED devices one has to consider more refined approaches in which, for example, NPs are placed close to the QW region and overgrown or are placed in the pockets of

#156569 - $15.00 USD Received 8 Nov 2011; revised 28 Dec 2011; accepted 2 Jan 2012; published 17 Jan 2012

nanopillar structure thus placing the NPs within the range of effective LSP coupling with QW region. The results of a recent work by Cho et al. [31] in which the authors placed the Ag NPs layer covered with SiO_2 nanodiscs in the p-GaN emitter and overgrew it with p-GaN shows the feasibility of the former approach. It is particularly interesting because the type of NPs they used to produce the LSP enhancement is closely related to the Ag/SiO_2 NPs analyzed in the present paper. Using the core/shell NPs in such an approach could provide additional benefits discussed above (suppression of NPs oxidation and coagulation) and also be advantageous in preventing defect formation in the overgrown layer due to the exclusion of direct contact of NPs with underlying and overgrowing GaN layers. Recently we have successfully tested another approach in which a nanopillar structure is formed in the n-GaN layer embedded with Ag NPs, and then overgrown with thin n-GaN, followed by the QW region and the p-GaN cap layer. Although the present experiments were called to demonstrate the feasibility of the principle and therefore were confined to samples with a thin undoped n-GaN cap instead of true LED structures, it should be possible to realize the efficient LSP coupling scheme in the regime of electrical injection by combining Ag/SiO_2-NPs with an electrically driven InGaN quantum well. All in all, we believe the Ag/SiO_2 core-shell LSP-enhanced MQW structure to be one of the possible paths to high efficiency stable LED structures.

Acknowledgments

This work was supported by the National Research Foundation of Korea (NRF) funded by the Korea government (MEST) (2010-0019626, 2010-0026614). J.-K. Yang acknowledges the support of the KOSEF through OPERA (R11-2003-22).

#156569 - $15.00 USD Received 8 Nov 2011; revised 28 Dec 2011; accepted 2 Jan 2012; published 17 Jan 2012